Investigation of Carbon Dioxide Corrosion of Mild Steel in the Presence of Acetic Acid—Part 1: Basic Mechanisms

K.S. George and S. Nešić‡,**

ABSTRACT

The corrosion behavior of mild steel in the presence of acetic acid (CH_3COOH) and carbon dioxide (CO_2) has been investigated using electrochemical techniques and weight-loss measurements. Electrochemical measurements have shown that the presence of acetic acid affects predominantly the cathodic reaction. The acetic acid effect is much more pronounced at elevated temperatures when catastrophic corrosion rates may be encountered at high concentrations. The undissociated form of acetic acid, present at lower pH, is responsible for the increases seen in the corrosion rate.

KEY WORDS: acetic acid, carbon dioxide corrosion, electrochemical techniques, mild steel, weight-loss measurements

INTRODUCTION

The presence of organic acids in oil and gas production and transport lines was first discovered in 1944 (for example, Crolet, et al.[1]). Classification of organic acids can be done on the basis of molecular weight, and it was found that the lower molecular weight organic acids were primarily soluble in water and can lead to corrosion of mild steel pipelines, as discussed below. Higher molecular weight organic acids are typically soluble only in the oil phase and pose a corrosion threat only at higher temperatures in the refineries. Even if the threat to mild steel pipelines posed by organic acids is well recognized today, the analysis of oilfield brines for the presence of organic acids is still not routinely done.

The following text will focus on the recent findings related to carbon dioxide (CO_2) corrosion of mild steel in the presence of acetic acid ([CH_3COOH] denoted as HAc in the text below), which is the most prevalent low molecular weight organic acid found in brines. However, a brief introduction to CO_2 corrosion will be given first.

Carbon Dioxide Corrosion

The corrosion mechanisms of CO_2 and its effects on mild steel under varying conditions of pressure, temperature, pH, and oil-water fractioning has been a widely researched topic. Some of the key studies include work by de Waard and coworkers,[2-5] Dugstad, et al.,[6] and Nešić and coworkers.[7-10] Furthermore, these authors have proposed models to predict CO_2 corrosion of mild steel based on the results of their work. The following is a summary of the key processes occurring in CO_2 corrosion.

Carbon dioxide gas dissolves in water and forms a "weak" carbonic acid through hydration by water:

$$CO_2(g) \Leftrightarrow CO_2 \quad (1)$$

$$CO_2 + H_2O \Leftrightarrow H_2CO_3 \quad (2)$$

The carbonic acid (H_2CO_3) then partially dissociates to form the bicarbonate ion, which can further dissociate to yield the carbonate ion:

Submitted for publication October 2005; in revised form, July 2006.

‡ Corresponding author. E-mail: nesic@ohio.edu.

* Institute for Corrosion and Multiphase Flow Technology, 342 West State St., Ohio University, Athens, OH 45701.

0010-9312/07/000023/$5.00+$0.50/0

© 2007, NACE International

$$H_2CO_3 \Leftrightarrow H^+ + HCO_3^- \quad (3)$$

$$HCO_3^- \Leftrightarrow H^+ + CO_3^{2-} \quad (4)$$

It is widely known that solutions containing H_2CO_3 are more corrosive to mild steel than solutions of strong acids, such as hydrochloric (HCl) or sulfuric (H_2SO_4), at the same pH. This was a topic of debate and speculation in the past few decades. de Waard and Milliams[2] suggested that this is due to the reduction of the undissociated H_2CO_3 molecule, which occurs after it is adsorbed onto the metal surface. According to them, this is the dominant and rate-determining step in the CO_2 corrosion process, so the corrosion rate of the mild steel surface is directly related to the concentration of the undissociated H_2CO_3 in solution and to the CO_2 partial pressure.

However, there are two possible cathodic reactions that can occur in the process of mild steel CO_2 corrosion: the above-mentioned "direct" reduction of H_2CO_3 but also reduction of hydrogen ions:

$$H_2CO_3 + e^- \Rightarrow H + HCO_3^- \quad (5)$$

$$H^+ + e^- \Rightarrow H \quad (6)$$

While the rate of the former process is determined by the amount of CO_2 in the system, the rate of the latter process is strongly pH-dependent. The electrons required to keep the process going are provided by a single anodic reaction, iron dissolution:

$$Fe \Rightarrow Fe^{2+} + 2e^- \quad (7)$$

Whether or not the direct reduction of H_2CO_3 (Reaction [5]) actually occurs on the metal surface was and still is a topic of debate, since it could be argued that undissociated H_2CO_3 is merely a source of hydrogen ions via Reaction (3) and would dissociate to give a hydrogen ion faster than it (carbonic acid) could diffuse to the surface of the steel. In this way H_2CO_3 would act as an additional source of hydrogen ions and lead to higher corrosion rates. Both pathways (Reactions [5] and [6]) release hydrogen gas from water as a product and, nowadays, it is accepted that direct reduction of H_2CO_3 (Reaction [5]) dominates at high partial pressures of CO_2 and high pH, while the reduction of hydrogen ions dominates at low CO_2 partial pressures and low pH.

When steel corrodes in CO_2-saturated water, the solubility of iron carbonate salt ($FeCO_3$) may be exceeded and precipitation sets in, which increases rapidly with the degree of supersaturation and an increase in temperature. The iron carbonate precipitate may form a protective film depending on the solution composition, pressure, and temperature of the system. Other solid corrosion products may form in the presence of chlorides, sulfides, oxygen, etc.

The effect of flow on CO_2 corrosion, when no protective films are present, is through increased mass transport of the corrosion species toward and away from the metal surface.[8] When the mass transport rate of the species (e.g., hydrogen ion) is not high enough to support the electrochemical process at the metal surface, limiting reaction rates are reached. On the other hand, species accumulation, supersaturation, and film precipitation can occur at the metal surface if the transport of the corrosion products (e.g., ferrous ions) away from the surface is not rapid enough. This is another mass-transfer effect of flow on CO_2 corrosion. However, flow may also affect the formation and survival of corrosion product films by mechanical means via hydrodynamic stresses.

Acetic Acid Corrosion

When HAc is present in the system it partitions between the aqueous and the gas phases. The aqueous HAc then partly dissociates into hydrogen and acetate ions:

$$HAc(g) \Leftrightarrow HAc \quad (8)$$

$$HAc \Leftrightarrow H^+ + Ac^- \quad (9)$$

Iron acetate salt can form in aqueous solutions; however, its solubility is much higher than that of iron carbonate, and therefore precipitation and protective film formation by iron acetate does not readily occur.

In 1999, Crolet, et al.,[1] described how low concentrations of HAc (6 ppm to 60 ppm) affect the corrosion rates of carbon steel. They argued that the increase in the rate of corrosion in the presence of HAc occurs due to an "inversion" in the bicarbonate/acetate ratio. At this inversion point, HAc is the predominant acid compared to H_2CO_3 and is therefore the main source of acidity. The work of Crolet, et al.,[1] also suggested that the presence of HAc inhibited the anodic (iron dissolution) reaction.

Hedges and McVeigh published results on the role of acetate in CO_2 corrosion.[11] Experiments using both HAc and sodium acetate as a source of acetate ions in various media (3% NaCl and two synthetic oilfield brines) were performed using rotating cylinder electrodes. Both sources of acetate ions were shown to increase the corrosion rate, but HAc decreased the pH while sodium acetate increased it. The increased corrosion rates were attributed to the formation of thinner iron carbonate films, since acetate ions have the ability to form iron acetate and transport iron away from the steel surface. However, no attempt was made to quantify the thickness or morphology of the films formed in their experiments. Little or no control of pH in their experiments may have led to the ambiguous effect of acetic species on corrosion. They also reported a mild increase in the cathodic reaction rate in the presence of HAc, but their results were not fully conclusive.

TABLE 1
Key Experimental Parameters

Steel Type	X-65
Aqueous solution	Oxygen-free, 3 wt% NaCl
Purged gas	CO_2, N_2
Total pressure	Atmospheric
HAc concentration	0 to 5,000 ppm
Temperature	22, 40, 60, 80°C
Rotation rate	100 rpm to 4,000 rpm
pH	4, 5, 6
Measurement techniques	Potentiodynamic sweeps (PS), linear polarization resistance (LPR), electrochemical impedance spectroscopy (EIS), weight loss (WL)

Some limited evidence on the role of HAc in CO_2 corrosion comes from field experience as related to the so-called top-of-line corrosion,[12] where HAc was said to have a detrimental effect.

Garsany, et al.,[13] used voltammetry to study the effect of acetate ions on the rates and mechanisms of corrosion with a rotating disc electrode (RDE) and film-free surfaces. Their voltammograms show two waves, which are attributed to the reduction of the hydrogen ion and "direct" HAc reduction on the steel surface:

$$HAc + e^- \Rightarrow H + Ac^- \quad (10)$$

They argue that, since HAc dissociation can occur very quickly, it is not possible to distinguish the reduction of hydrogen ions (Reaction [6]) from direct HAc reduction (Reaction [10]) at the electrode surface.

Joosten, et al.,[14] performed experiments using HAc, synthetic seawater, and an oil phase in glass cells. They found that HAc increased the corrosion rate by decreasing the pH, but the system could be inhibited very effectively (below 400 ppm HAc). Effective inhibition has also been reported by Hedges and McVeigh.[11]

Generally speaking, very few systematic studies have been performed in the laboratory. Consequently, little or no information exists regarding the basic effect of HAc on the anodic and cathodic reactions as outlined above.

Based on previous research, some of the principal questions still need to be answered:

1. What are the main effects of HAc on the CO_2 corrosion process? Does HAc interfere with the anodic and cathodic reactions otherwise present in CO_2 corrosion or does it lead to new additional electrochemical reactions at the steel surface? How big is the effect?
2. Does anything change at high pressures and temperatures?
3. Is there an effect of HAc on the formation of protective iron carbonate films?
4. What is the best way to integrate the findings about the HAc effect on CO_2 corrosion into a corrosion prediction model?

The first point is the topic of the present paper. Effects of HAc at high pressures and temperatures, protective film formation and modeling are subjects of separate papers.

EXPERIMENTAL PROCEDURES

The test matrix described in Table 1 was executed in order to seek answers to the first question posed above.

All of the permutations of the parameters in the experimental matrix were not performed. When one parameter was varied, the other parameters were set to their baseline values, which were selected to be: 1 bar CO_2, 22°C, 100 ppm total aqueous acetic species, pH 4, and 1,000 rpm. For example, in the HAc concentration study, the HAc concentration was varied from 0 to 5,000 ppm, but the temperature remained constant at 22°C. The system pH was maintained at 4 and the rotational velocity was kept at 1,000 rpm. In this way effects of various parameters were deconvoluted. This is particularly important for parameters that are closely linked, such as HAc concentration and pH.

It should be noted that in this part of the study the key parameters (listed in Table 1), such as pH and temperatures, have been chosen to yield conditions where corrosion product film formation is unlikely or very slow. This enabled a more accurate study of the underlying electrochemical processes, mass-transfer, and water chemistry effects. The weight-loss experiments, for similar reasons, were performed over short periods of time (typically 24 h) to avoid any significant film formation.

EXPERIMENTAL SETUP

A schematic of the experimental cell is shown in Figure 1. To begin, the experimental apparatus was assembled. A salt solution was prepared, added to the cell, and then deoxygenated for at least 1 h using nitrogen or CO_2 gas. The test temperature was set using a hot plate and controlled using a feedback temperature probe. Once deoxygenation had occurred and the test temperature was reached, the appropriate amount of HAc was then added to the cell and deoxygenation was continued for an additional 30 min. Since HAc is somewhat volatile, bubbling pure CO_2 gas through the solution would strip the HAc out of the test cell. A gas "preconditioning" cell was used as a remedy. The preconditioning cell was kept constant at the test temperature and contained the same fluid composition as the experimental cell. The preconditioning cell ensured the CO_2 entering the experimental cell was saturated with HAc and H_2O vapor and that

the HAc stripping occurred much slower and could therefore be ignored.

The pH meter used in the experiments was calibrated at the test temperature by heating the buffer solutions. The pH was monitored and adjusted before and after the HAc addition to ensure the fluid composition was similar between test runs. To achieve the desired system pH, minute adjustments were made using droplets of hydrochloric acid or sodium bicarbonate ($NaHCO_3$) solutions.

The working electrode had a 120-cm diameter and an area of 5.4 cm^2. The composition of the X-65 mild steel used in the experiments is shown in Table 2. The cylindrical electrode was polished using 600-grit sand paper, copiously washed with ethanol (C_2H_6O), dried, immersed into the test solution, and the electrode's rotational velocity was set. After approximately 30 additional minutes, electrical connections were made and electrochemical measurements started.

A concentric platinum wire ring was used as a counter electrode and a silver/silver chloride (Ag/AgCl; 3 M potassium chloride [KCl]) external electrode connected with the cell via a salt bridge and a Luggin capillary served as a reference electrode. The electrochemical measurements were typically conducted in the same order:

—Corrosion rate was measured using linear polarization resistance (LPR).
—Solution resistance was found using electrochemical impedance spectroscopy (EIS).
—Cathodic and then the anodic potentiodynamic sweeps were performed.

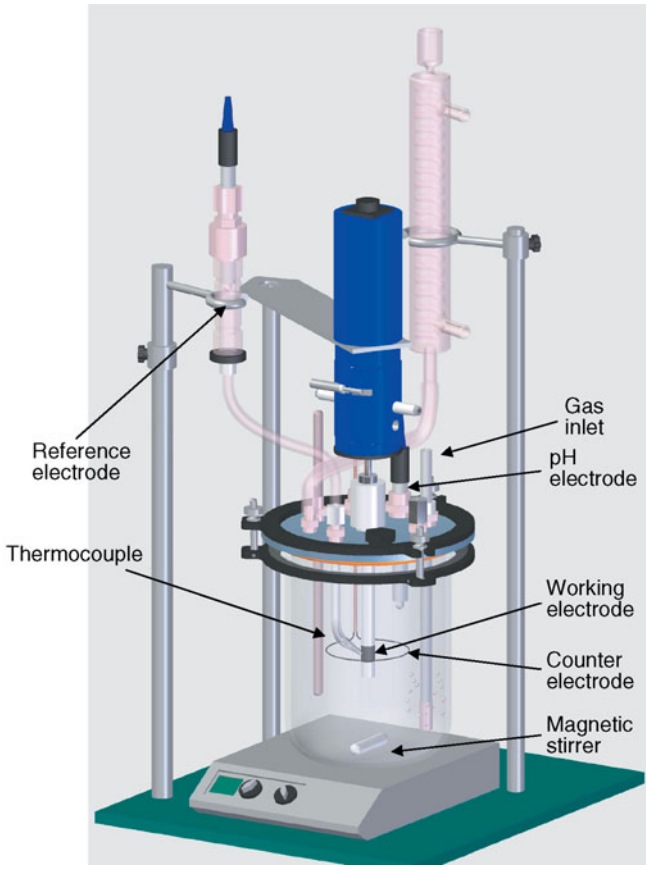

FIGURE 1. *Schematic of the test cell.*

Electrochemical Measurements

All electrochemical measurements were made using a potentiostat. The potentiodynamic polarization curves (sweeps) were conducted at a scan rate of 0.2 mV/s, and the potential was manually corrected for solution resistance, which was measured using EIS. Potentiodynamic sweeps were conducted at constant pH with the pH adjustment occurring after each sweep. During the anodic sweep, for example, the system pH was set to 4 and the sweep started. Due to iron dissolution, the pH of the system would rise to 4.08 by the end of the sweep. As ferrous ions are rapidly generated on the working electrode, hydrogen ions and water are reduced on the counter electrode, releasing the hydroxide ions into the solution. This leads to an increase in the bulk pH. After the anodic sweeps, the pH was then adjusted using HCl before the beginning of the next sweep. Anodic sweeps were limited to polarization less than 200 mV above the corrosion potential to limit buildup of excessive ferrous concentrations in the test cell.

The potentiodynamic sweeps were always conducted starting from the corrosion potential. For example, a cathodic potentiodynamic sweep would scan from the corrosion potential to approximately –650 mV below the corrosion potential. The corrosion potential would then be allowed to drift back to the starting corrosion potential before an anodic potentiodynamic sweep was performed. The LPR measurements were taken at ±5 mV around the corrosion potential, by using a potentiodynamic scan at 0.1 mV/s.

TABLE 2
Chemical Composition of API 5LX65 Steel (wt%)

Al	Cr	Mo	S	V	B	Cu	Nb	Si
0.032	0.011	0.103	0.004	0.055	0.0002	0.010	0.030	0.240
C	**Fe**	**Ni**	**Sn**	**Ca**	**Mn**	**P**	**Ti**	
0.150	Balance	0.020	0.005	0.0032	1.340	0.011	0.001	

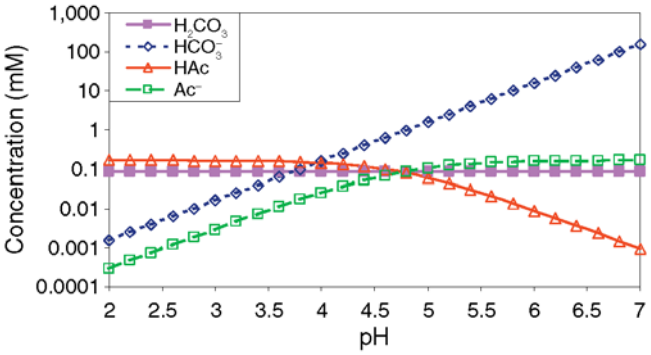

FIGURE 2. *The effect of pH on the concentration of species at 1 bar CO_2, 22°C, when 10 ppm HAc was added.*

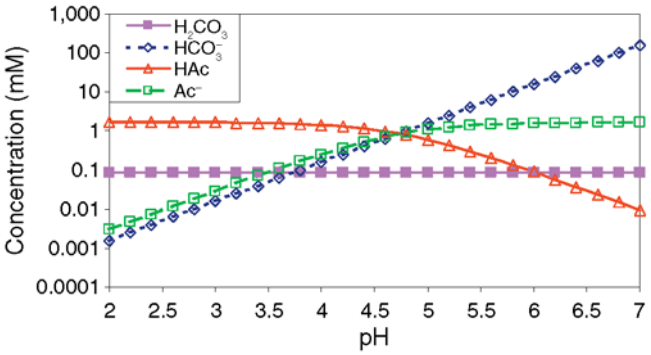

FIGURE 3. *The effect of pH on the concentration of species at 1 bar CO_2, 22°C, when 100 ppm HAc was added.*

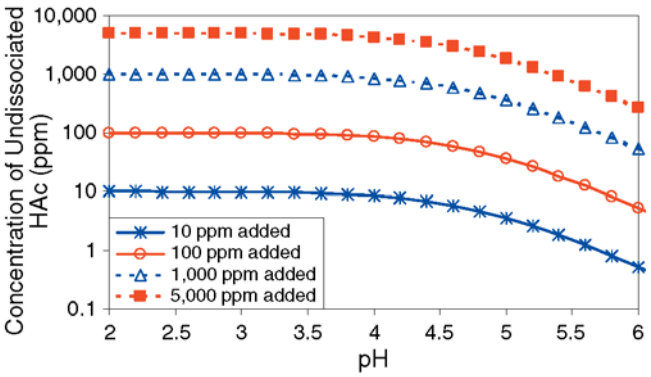

FIGURE 4. *The concentration of undissociated aqueous HAc as a function of system pH at 22°C for various amounts of HAc added.*

Weight-Loss Experiments

In a separate series of weight-loss experiments, after the solution had come to the desired temperature and the pH was adjusted, a preweighed steel sample was immersed into the solution. During the 24-h weight-loss experiments, the pH was adjusted approximately every hour or two, which corresponded with the procedure used in the LPR measurements. After 24 h, the electrodes were taken out of the test solution, rinsed with alcohol, wiped with a soft cloth to remove any corrosion product, and then weighed after drying.

RESULTS AND DISCUSSION

Water Chemistry Calculations

The water chemistry of the experimental solutions was found by solving the equilibrium expressions for the reactions given above (1, 2, 3, 4, 8, and 9). Expressions for the equilibrium constants are the same as those used in the mechanistic model of Nešić, et al.[10] The concentrations of some of the key species at 1 bar CO_2, 22°C, when 10 ppm HAc (total) is added, are shown in Figure 2. The concentration of dissolved CO_2 and H_2CO_3 is fixed with the partial pressure of the purged gas and is not a function of pH. As most of the experimental work was performed at pH 4, it is evident that when 10 ppm HAc is added to the solution, HAc is the main source of acidity up to a pH of approximately 4.7. When 100 ppm HAc is added, under the same conditions, it is the main source of acidity up to a pH of almost 6. This is shown in Figure 3.

In the results presented below, the concentration of HAc will be reported as both the total amount of HAc added to the system as well as the amount of aqueous "free" HAc that stayed in undissociated form. For example, when 100 ppm HAc was added to the system and the pH adjusted to 4, the free concentration of HAc was 85 ppm, but when experiments were performed at pH 6 the same addition of 100 ppm of HAc to the system resulted in a free HAc concentration of only 6 ppm. The undissociated concentration of HAc as a function of pH is shown in Figure 4.

Effect of HAc Concentration

In the first series of experiments, potentiodynamic sweeps were performed in 3 wt% NaCl solutions purged with nitrogen for an undissociated HAc concentration range from 0 to 850 ppm (obtained by adding 0 to 1,000 ppm of HAc at pH 4). Nitrogen is inert and was used to remove any interference from CO_2 so that the effect of HAc could be seen more clearly. Normally, addition of HAc reduces the pH; however, the pH was held constant in these experiments (by adding HCl) to distinguish the effect of the acetic species from the effect of hydrogen ion concentration on the cathodic and anodic reactions. At a constant pH, the concentration of hydrogen ions is fixed, and the effect of the acetic species on the cathodic and anodic reactions could be distinguished. The HAc concentration range was selected to represent situations typically encountered in service.

From Figure 5 it can be seen that at room temperature there is a clear increase of the cathodic limiting current density with increased concentrations of HAc. When the concentration of HAc increased from 0 to 850 ppm, the limiting current density increased almost 30 times. In the absence of HAc, the limiting

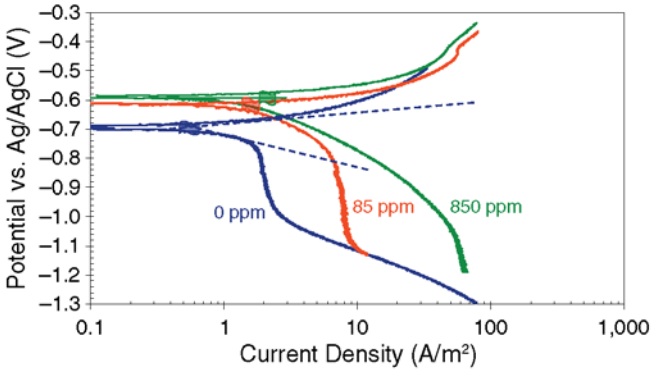

FIGURE 5. *Potentiodynamic polarization curves done on X65 steel corroding in aqueous solutions purged with N_2 at pH 4, 1,000 rpm, 22°C, containing various amounts of undissociated aqueous HAc (0, 100 ppm, and 1,000 ppm total acetic species, respectively). The dashed lines are estimated Tafel lines, which are extrapolated to the corrosion potential to determine the corrosion rate. The shaded areas represent a range of values of the corrosion current and corrosion potential as determined by LPR (Figure 6).*

current arises from diffusion of hydrogen ions. The increase of the limiting current in the presence of HAc was related to the diffusion of undissociated HAc as discussed below. It may appear that under these conditions the anodic reaction was retarded in the presence of HAc, as reported by Crolet, et al. However, this conclusion must be taken with caution as the changes in the anodic portion of the curves were overshadowed by the large changes in the cathodic reaction, which resulted in a large change of the corrosion potential. The corrosion rate increased only by a factor of 2 to 3 under the same conditions, as shown in Figure 6. Comparison of the corrosion rates measured by LPR and estimated by Tafel extrapolation shown in Figure 6 suggests that the values obtained by the two techniques are close, considering the inherent errors with using these techniques. By assuming charge-transfer control, a cathodic Tafel slope of 120 mV/decade and an anodic Tafel slope of 40 mV/decade (determined from Figure 5) were used in both methods. The values of the estimated corrosion current by using LPR are overlaid on the potentiodynamic curves in Figure 5. It is clear that corrosion currents were in all cases much lower than the cathodic limiting currents (by an order of magnitude or more), confirming that the corrosion process is charge-transfer-controlled under these conditions.

In a subsequent series of experiments, the aqueous solution was purged with CO_2 and the HAc concentration was varied from 0 to 850 ppm of undissociated HAc (corresponding to 1,000 ppm total acetic species at pH 4). The resulting cathodic and anodic sweeps are shown in Figure 7. The effect of HAc concentration on the corrosion rate is shown in Figure 8. As in the case described above without CO_2, the limiting current of the cathodic reaction in the pres-

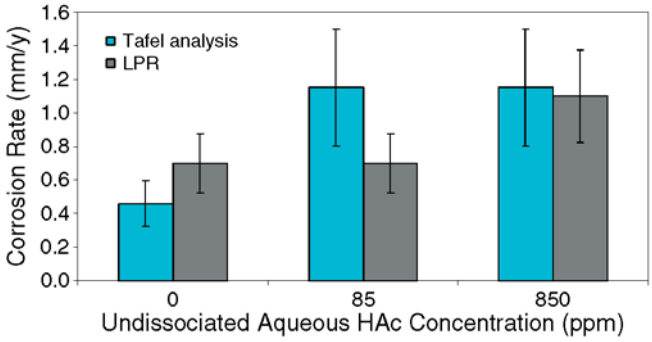

FIGURE 6. *The effect of HAc concentration on the corrosion rate of X65 steel in aqueous solutions purged with N_2 at pH 4, 1,000 rpm, 22°C, as measured by the LPR and Tafel extrapolation techniques (Figure 5). The error bars represent minimum and maximum values obtained in repeated experiments.*

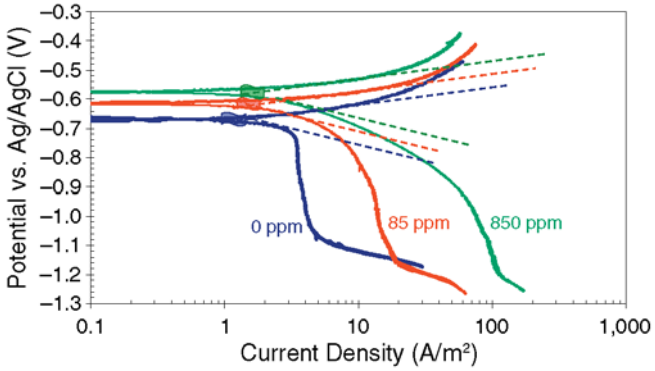

FIGURE 7. *Potentiodynamic polarization curves done on X65 steel corroding in aqueous solutions purged with CO_2 at pH 4, 1,000 rpm, 22°C, containing various amounts of undissociated aqueous HAc (0, 100 ppm, and 1,000 ppm total acetic species, respectively). The dashed lines are estimated Tafel lines, which are extrapolated to the corrosion potential to determine the corrosion rate. The shaded areas represent the range of values of the corrosion current and corrosion potential as determined by LPR (Figure 8).*

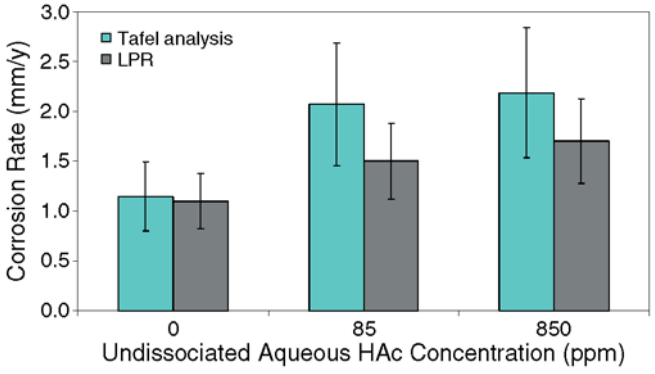

FIGURE 8. *The effect of HAc concentration on the corrosion rate of X65 steel in aqueous solutions purged with CO_2 at pH 4, 1,000 rpm, 22°C, as measured by the LPR and Tafel extrapolation techniques (Figure 7). The error bars represent minimum and maximum values obtained in repeated experiments.*

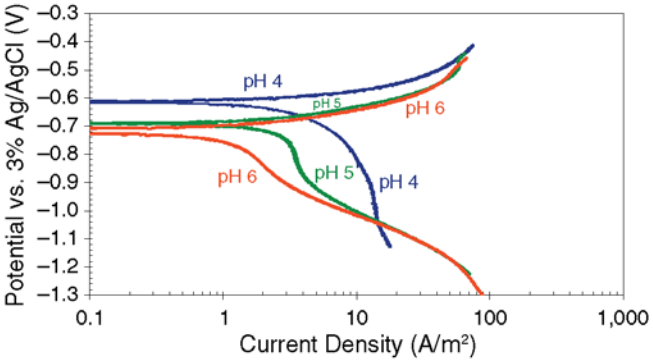

FIGURE 9. *The effect of pH on potentiodynamic sweeps done on X65 steel corroding in aqueous solutions purged with CO_2 containing 100 ppm total acetic species at 1,000 rpm, 22°C.*

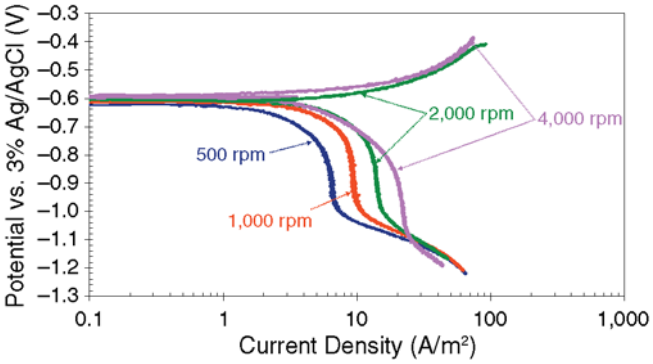

FIGURE 10. *The effect of rotational velocity on potentiodynamic polarization curves done on X65 steel corroding in aqueous solutions purged with CO_2 containing 100 ppm total acetic species (85 ppm undissociated HAc at pH 4), 22°C.*

ence of CO_2 was greatly increased with increasing concentrations of HAc. On the other hand, the corrosion current/rate approximately doubled when HAc was present. In pure CO_2 corrosion (0 ppm HAc) the corrosion current was of a similar order of magnitude as the limiting current, suggesting mixed charge/chemical control. However, in the presence of HAc the corrosion current was at least an order of magnitude smaller than the limiting current, suggesting pure charge-transfer control. The anodic Tafel slope was found to be 60 mV/decade to 80 mV/decade when CO_2 was present, suggesting a slight change in mechanism for iron dissolution. The cathodic Tafel slope remained 120 mV/decade. The presence of HAc did not change the situation. Using these Tafel slopes the corrosion rates calculated by LPR and the Tafel extrapolation agreed within the error of measurement.

When comparing the case without CO_2 (Figures 5 and 6) to the case that includes CO_2 (Figures 7 and 8), it is seen that both the limiting current and the corrosion current/rate are larger for the latter case with CO_2. Clearly, the presence of CO_2 introduces an additional corrosive species: undissociated carbonic acid (Reaction [5]).

Effect of pH

The effect of pH on the potentiodynamic polarization curves was studied in solutions saturated with CO_2 with the addition of 100 ppm HAc adjusted in the pH range from 4 to 6. The results are shown in Figure 9. As the pH is increased from 4 to 5, the anodic reaction rate is increased, consistent with Bockris's iron dissolution mechanism.[15] However, a further increase in pH from 5 to 6 did not result in a further increase in the anodic reaction rate. On the other hand, the cathodic reaction and particularly the limiting current was retarded by an increase in the pH. This is expected, since with the increase of the pH the concentration of the hydrogen ion decreases, but also because the concentration of undissociated HAc decreases with pH increase (Figure 3).

Effect of Rotational Velocity

The effect of velocity was studied by using potentiodynamic sweeps performed in 3% NaCl solution, saturated with CO_2 with the addition of 100 ppm HAc (85 ppm undissociated HAc at pH 4), 22°C. The results are shown in Figure 10. The increase in the limiting current is measured to be approximately a factor of 1.8 to 2 for every doubling of velocity, which is in excellent agreement with the mass-transfer theory. One can conclude that in HAc solution the reduction process is limited by the mass transfer of acetic species (probably undissociated HAc). In contrast, the limiting currents seen in pure CO_2 corrosion are chemical reaction-controlled (arising from a slow CO_2 hydration step, Reaction [2]) and exhibit a weak flow dependence.[16-17] The corrosion potential, as well as the anodic reaction, do not change with velocity, suggesting pure charge-transfer corrosion process under these conditions and a constant corrosion rate unperturbed by velocity.

Effect of Temperature

The effect of temperature on the potentiodynamic sweeps was studied in 3% NaCl solutions saturated with CO_2 with the addition of 100 ppm HAc (85 ppm undissociated HAc at pH 4), 1,000 rpm. The results are shown in Figure 11. There is a clear acceleration of both the cathodic and anodic reaction rates with an increase in temperature, as is expected. The corrosion rate, which is under charge-transfer control at room temperature (22°C), becomes mass-transfer limiting current controlled at higher temperatures. The corrosion rates measured by LPR and calculated from Tafel slopes were in good agreement.

Repeatability of the Potentiodynamic Sweeps

To put the results presented above into a proper perspective, a single baseline experiment was performed multiple times to estimate the repeatability. The repeatability was rather good, and the changes seen on the plots presented above are genuine and do

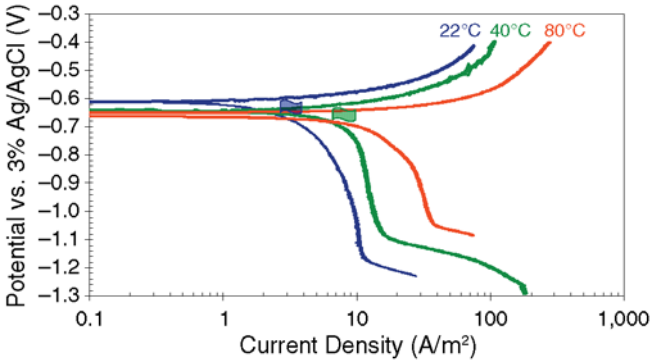

FIGURE 11. *The effect of temperature on potentiodynamic polarization curves done on X65 steel corroding in aqueous solutions purged with CO_2 containing 100 ppm total acetic species (approximately 85 ppm undissociated HAc at pH 4), 1,000 rpm. The shaded areas represent the range of values of the corrosion current and corrosion potential as determined by LPR.*

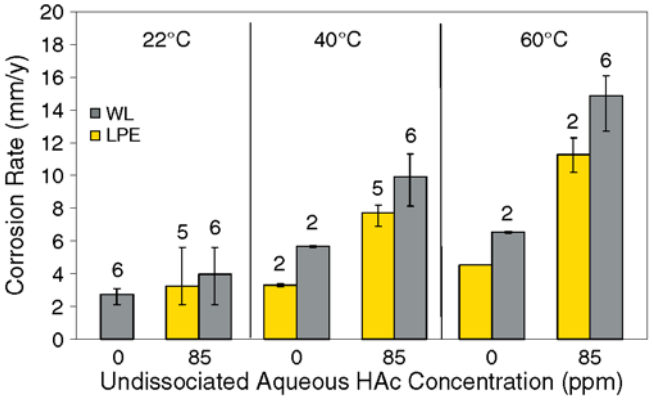

FIGURE 12. *The effect of temperature and HAc concentration on the corrosion rate of X65 steel in aqueous solutions purged with CO_2 at pH 4, 1,000 rpm, as measured by the LPR and weight-loss (WL) techniques. The error bars represent minimum and maximum values obtained in repeated experiments and the figure above the bars is the number of repeats.*

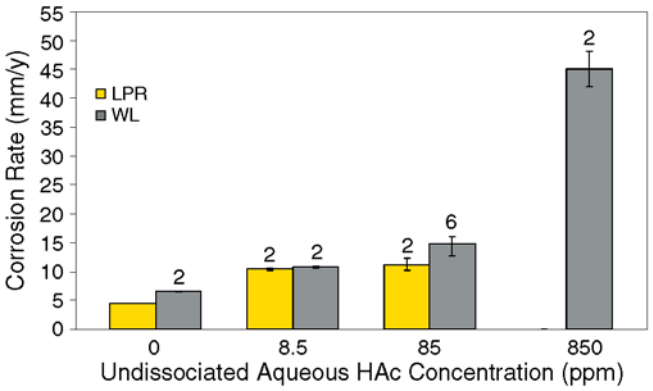

FIGURE 13. *The effect of HAc concentration on the corrosion rate of X65 steel in aqueous solutions purged with CO_2 at 60°C, pH 4, 1,000 rpm, as measured by the LPR and weight-loss (WL) techniques. The error bars represent minimum and maximum values obtained in repeated experiments and the figure above the bars is the number of repeats.*

reflect influences of various parameters beyond the experimental error.

Verification—Weight-Loss Experiments

A series of weight-loss experiments was conducted to verify the effect of HAc on the CO_2 corrosion of carbon steel in 3% NaCl solutions. The results are shown in Figure 12. The average value of the corrosion rate obtained by the weight-loss method is presented in the form of solid bars, while the error bars represent the maximum and minimum experimental values obtained in "repeated" experiments. The number above the error bars represents the number of repeated experiments used to calculate the average value. The values presented for the LPR method are time-averaged over the course of the experiment. In most experiments weight loss and LPR were done on the same specimen; however, in a few experiments no electrochemical experimentation was done to see if, by measuring the corrosion rate using LPR, the system was disturbed enough to change the corrosion rate measured by weight loss. No interference was found.

The effect of increasing temperature on the corrosion rate as measured by weight loss and LPR in 3% NaCl solutions without HAc and solutions where 100 ppm HAc was added (85 ppm undissociated HAc at pH 4, 22°C) is shown in Figure 12. It is evident that the corrosion rates measured using LPR and by weight loss are not in perfect agreement, even when HAc is not present. Nevertheless, the changes in corrosion rate observed with HAc concentration and temperature are significant when compared to the error measured for each technique individually. It appears that as the temperature increases, the influence of HAc is more pronounced. For example, at 22°C, adding 100 ppm HAc increases the corrosion rate approximately 30%, while at 60°C, the same increase in HAc concentration doubles the corrosion rate. If one converts the corrosion rates obtained at 40°C, shown in Figure 12, into corrosion currents (approximately 8 A/m^2 to 10 A/m^2) and compares them with the cathodic limiting current observed under the same conditions, shown in Figure 11 (which are approximately 10 A/m^2), this confirms that at elevated temperatures the corrosion process is under mass-transfer control.

The temperature effect was investigated further by looking at the effect of adding various amounts of HAc at 60°C to a 3% NaCl solution at pH 4 (Figure 13). It is evident that even a 10-ppm HAc addition to the solution affects the corrosion rate at 60°C, while adding 1,000 ppm leads to catastrophic corrosion rates. It is worth noting that the 1,000-ppm HAc, 24-h weight-loss experiment was performed four times. In

two of the tests, weight-loss measurements on the order of approximately 45 mm/y were observed, and these results are presented in Figure 13. In the other two experiments, the samples experienced some pitting corrosion. No discernable difference between the four experiments can be found to identify the trigger for the pitting corrosion.

Summary of Findings

From all of the above it appears that the key effect of HAc on the CO_2 corrosion of carbon steel is to introduce an additional cathodic species into the solution. All the results point to the same conclusion: this additional corrosive species is the undissociated HAc. The additional cathodic reaction (Reaction [10]) appears to be under charge-transfer control at room temperature, while at higher temperatures it becomes mass-transfer-controlled. Consequently, the presence of HAc is a problem predominantly at high temperatures and at low pH, where the concentration of undissociated HAc is high.

CONCLUSIONS

❖ Electrochemical measurements have shown that the presence of HAc strongly affects the cathodic limiting current, which is mass-transfer-controlled. The anodic reaction (iron dissolution) was unaffected or mildly retarded with increasing HAc concentration at room temperature.

❖ At room temperature the CO_2 corrosion rate of carbon steel is only mildly affected by the presence of HAc. At 22°C the corrosion process seems to be under charge-transfer control and unaffected by flow.

❖ As the temperature increases, the HAc effect is much more pronounced and much higher corrosion rates are obtained. It seems that HAc corrosion becomes mass-transfer-controlled at elevated temperatures, making it more prone to flow effects.

❖ It appears that the undissociated form of HAc is the key species primarily responsible for changes seen in the mild steel corrosion process.

ACKNOWLEDGMENTS

During this work, K.S. George has been supported by a grant from the Ohio University's Stocker Fund. The authors would like to acknowledge the contribution of a consortium of companies whose continuous financial support and technical guidance enabled this work. They are BP, Champion Technologies, Clariant, ConocoPhillips, ENI, MI Technologies, Ondeo Nalco, Saudi Aramco, and Total.

REFERENCES

1. J.-L. Crolet, N. Thevenot, A. Dugstad, "Role of Free Acetic Acid on the CO_2 Corrosion of Steels," CORROSION/1999, paper no. 24 (Houston, TX: NACE International, 1999).
2. C. de Waard, D.E. Milliams, Corrosion 31, 5 (1975): p. 175.
3. C. de Waard, U. Lotz, D.E. Milliams, Corrosion 47, 12 (1991): p. 976.
4. C. de Waard, U. Lotz, "Prediction of CO_2 Corrosion in Carbon Steel," CORROSION/1993, paper no. 69 (Houston, TX: NACE, 1993).
5. C. de Waard, U. Lotz, A. Dugstad, "Influence of Liquid Flow Velocity on CO_2 Corrosion: A Semi-Empirical Model," CORROSION/1995, paper no. 128 (Houston, TX: NACE, 1995).
6. A. Dugstad, L. Lunde, K. Videm, "Parametric Study of CO_2 Corrosion of Carbon Steel," CORROSION/1994, paper no. 14 (Houston, TX: NACE, 1994).
7. S. Nešić, G.T. Solvi, J. Enerhaug, Corrosion 51, 10 (1995): p. 773.
8. S. Nešić, J. Postlethwaite, S. Olsen, Corros. Sci. 52, 4 (1996): p. 280.
9. S. Nešić, B.F.M. Pots, J. Postlethwaite, N. Thevenot, J. Corros. Sci. Eng. 1, paper no. 3 (1995).
10. S. Nešić, M. Novdsveen, R. Nyborg, A. Stangeland, "A Mechanistic Model for CO_2 Corrosion with Protective Iron Carbonate Films," CORROSION/2001, paper no. 01040 (Houston TX: NACE, 2001).
11. B. Hedges, L. McVeigh, "The Role of Acetate in CO_2 Corrosion: The Double Whammy," CORROSION/1999, paper no. 21 (Houston TX: NACE, 1999).
12. Y.M. Gunaltun, D. Larrey, "Correlation of Cases of Top of Line Corrosion with Calculated Water Condensation Rates," CORROSION/2000, paper no. 71 (Houston, TX: NACE, 2000).
13. Y. Garsany, D. Pletcher, B. Hedges, "The Role of Acetate in CO_2 Corrosion of Carbon Steel: Has the Chemistry Been Forgotten?" CORROSION/2002, paper no. 02273 (Houston, TX: NACE, 2002).
14. M.W. Joosten, J. Kolts, J.W. Hembree, M. Achour, "Organic Acid Corrosion in Oil and Gas Production," CORROSION/2002, paper no. 02294 (Houston, TX: NACE, 2002).
15. J.O'M. Bockris, A.K.N. Reddy, Modern Electrochemistry (New York, NY: Plenum Press, 1973).
16. G. Schmitt, B. Rothman, Werkst. Korros. 28 (1977): p. 816.
17. S. Nešić, B.F.M. Pots, J. Postlethwaite, N. Thevenot, J. Corros. Sci. Eng. (1995).